Bismuth Zinc Vanadate, $BiZn_2VO_6$: New Crystal Structure Type and Electronic Structure

Sayonara Eliziario Nunes[a,b], Chun-Hai Wang[a], Karwei So[a], John S. O. Evans[a] and Ivana Radosavljević Evans[a*]

[a] *Department of Chemistry, Durham University, South Road, Durham. DH1 3LE, UK*

[b] *Department of Materials Engineering, Federal University of São Carlos, 13565-905, São Carlos, SP, Brazil*

*Email: ivana.radosavljevic@durham.ac.uk

Abstract

We report a combined experimental and computational study of the crystal structure and electronic properties of bismuth zinc vanadate, $BiZn_2VO_6$, known for its visible light photocatalytic activity. The crystal structure has been solved from laboratory powder X-ray diffraction data using the repeated minimisations from random starting values method. $BiZn_2VO_6$ adopts a new structure type, based on the following building blocks: corner- and edge-sharing ZnO_4 tetrahedra, ZnO_6 octahedra and VO_4 tetrahedra, and Bi_2O_{12} dimers. It is the only known member of the BiM_2AO_6 (M = Pb, Ca, Cd, Mn, Zn, Mg, Cu; A = V, P, As) family which does not appear to be structurally closely related to others. The electronic structure of $BiZn_2VO_6$, calculated by DFT methods, shows that it is an indirect gap semiconductor with a calculated band gap of 1.6 eV, which compares favourably to the experimentally measured value of 2.4 eV.

1. Introduction

Mixed metal oxides with the general formula BiM_2AO_6 (M = Mg, Ca, Cd, Cu, Pb, Mn, Zn; A = V, P, As) form a family of materials with rich structural chemistry and physical properties.[1-15] Interesting properties of the BiM_2VO_6 compounds include non-linear optical behaviour [5, 10], low-dimensional spin-ladder magnetism [16, 17] and photocatalytic activity for organic dye degradation and oxygen evolution.[18-20]

The crystal structures of these materials can be generally described as based on orthorhombic unit cells of approximate dimensions a ~ 11.5 Å, b ~ 5.5 Å and c ~ 8.5 Å, and typically contain BiO_2^- infinite chains, AO_4 tetrahedra and interspersed M^{2+} cations which, depending

on the size and bonding preferences, adopt coordination numbers between 5 and 7. Seven vanadates with the above general formula have been reported, with M = Mg, Ca, Cd, Cu, Pb, Mn and Zn, and full structures have been reported for all except the Zn compound. The known structures are closely related and can be described in terms of the building blocks mentioned above. $BiMg_2VO_6$ and $BiMn_2VO_6$ both crystallise in space group Pnma, with the former undergoing a phase transition to Cmcm at about 300 K. [8, 12] $BiCa_2VO_6$ and $BiCd_2VO_6$ adopt the noncentrosymmetric polar space group $Cmc2_1$. [5, 9] $BiCu_2VO_6$ and $BiPb_2VO_6$ are both primitive monoclinic at room temperature and undergo phase transitions to higher symmetry structures at high temperatures. [11, 14] The synthesis of $BiZn_2VO_6$ was reported by Bosacka *et al.*, who reported an indexed powder diffraction pattern and a triclinic unit cell, but no further structural information was given. [21]

In this paper we report a combined experimental and computational study of the structure and properties of $BiZn_2VO_6$. We show that $BiZn_2VO_6$ adopts an entirely new structure type and that it is the only material in the BiM_2AO_6 (A = V, P, As) family which doesn't appear to be structurally closely related to others. We also report electronic structure calculations performed on $BiZn_2VO_6$ by DFT.

2. Experimental

2.1 Synthesis

All polycrystalline samples were prepared from stoichiometric quantities of Bi_2O_3, ZnO, CuO and NH_4VO_3, by heating an intimately ground mixture of the reagents in alumina crucibles in air at 700^{o}C and 800^{o}C for 30 hours at each temperature, with grinding between the two firings.

2.2 Structural characterisation

Powder X-ray diffraction (PXRD) data were collected on a Bruker D8 ADVANCE diffractometer, with Cu$K\alpha_1$ radiation equipped with a VÅNTEC position sensitive detector. PXRD data for the initial structure solution of $BiZn_2VO_6$ were collected in a 10-90° 2θ range, with a step size of 0.02° and a step time of 3 s, while the data set for the refinement was carried out using a pattern collected in a 10-120° 2θ range, with a step size of 0.02° and a step time of 5 s. All PXRD data were analysed using Topas Academic software. [22]

2.3 Electronic structure calculations

To analyse the structure and the electronic properties of $BiZn_2VO_6$ from a theoretical aspect, we conducted first-principle calculations using the CASTEP (Cambridge Serial Total Energy Package) software-package.[23] For the calculations, a plane wave basis set with a cut-off energy E_{cut} = 500 eV was chosen for expansion of valence-electron wave functions at the Local Density Approximation (LDA) level. The structure obtained experimentally in the current work was used as a starting model. A further geometry optimisation by the Broyden-Fletcher-Goldfarb-Shannon (BFGS) method was performed. The criterion for self-consistency (SCF) was eigenenergy convergence within 10^{-9} eV/atom. The k-space was sampled using a 5×5×4 Monkhorst-Pack grid (reciprocal spacing ~0.04 $Å^{-1}$) and the ultrasoft pseudopotential was constructed from the CASTEP database. For the geometry optimisation, the convergence criterion was set as absolute net force within 10^{-3} eV/Å. Finally, the electronic band structure of the optimised structure was calculated using the same electronic SCF parameters.

3. Results and discussion

3.1 Crystal structure of $BiZn_2VO_6$

The structure solution of $BiZn_2VO_6$ was carried out by repeated minimisations from random starting values implemented in Topas Academic. The observed PXRD pattern was Pawley fitted [24] using the triclinic unit cell proposed by Bosacka *et al*. [21] and space group P−1. The obtained cell parameters were: a = 6.88278(8) Å, b = 5.72909 (6) Å, c = 8.9059(1) Å, α = 90.988(1)^o, β = 130.130(1)^o and γ = 99.547(1)^o, V = 261.171(6) $Å^3$. Once a satisfactory Pawley fit was obtained (R_{wp} = 2.20%), the unit cell parameters, the zero point, the peak shape function terms and the background terms were fixed. The unit cell volume, the space group and the formula suggested that the asymmetric unit should consist of 1 Bi, 2 Zn, 1 V and 6 O atoms, assuming they were all located on the general position. The starting configuration for structure solution was an asymmetric unit in which all 10 crystallographically independent atoms were placed at the origin, with an overall isotropic atomic displacement parameter B_{iso} = 1 $Å^2$; this configuration corresponds to an agreement factor R_{wp} = 29.25%. Repeated minimisations from random starting values [25] were performed during which the fractional coordinates of the 10 unique atoms were varied (randomly displaced, then optimised by Rietveld refinement), along with one overall isotropic temperature factor. This approach repeatedly produced a solution which gave an excellent fit

to the experimental pattern (R_{wp} = 3.57%) and a physically sensible model consisting of a tetrahedrally coordinated V atom and one tetrahedral and one distorted octahedral Zn atom. Free Rietveld refinement [26] of this starting model was carried out against the full data set (10-120° 2θ range), in which the varied parameters included the zero point, background terms, the peak shape function terms, the fractional coordinates of all atoms and two isotropic atomic displacement parameters (one for the metals and one for the oxygen atoms). This gave an excellent fit to the observed data, with R_{wp} = 2.70%, the V-O bond lengths ranging from 1.60–1.81 Å, tetrahedral Zn-O bond lengths ranging from 1.91–2.03 Å and octahedral Zn-O bond lengths from 1.88–2.35 Å. Applying bond length restraints led to a narrower spread of bond lengths with a very small increase in the R-factor (R_{wp} = 2.81%, Rietveld plot shown in Figure 1); this is the final crystallographic model presented in Table 1 and Table 2.

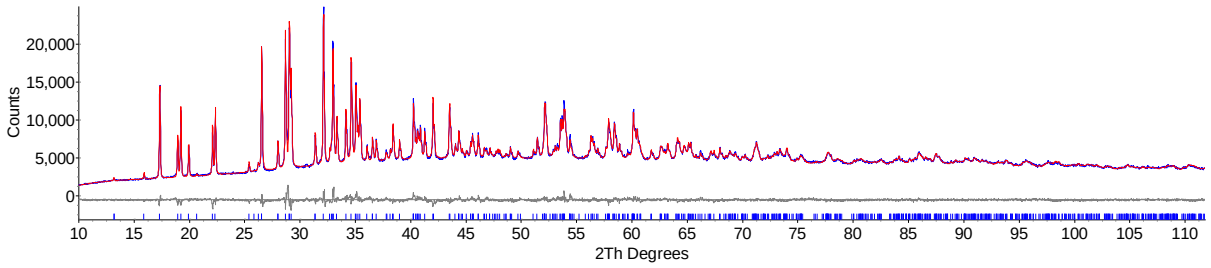

Figure 1. The final Rietveld refinement plot for $BiZn_2VO_6$: observed data in blue, calculated pattern in red, difference curve in grey. R_{wp} = 2.81%, R_{Bragg} = 1.44%.

The structure of $BiZn_2VO_6$ is shown in Figure 2. Bi atoms are found in an irregular coordination environment, typical of a lone-pair cation, with three shorter (2.20 – 2.42 Å) and four longer (2.78 – 2.90 Å) bonds. Pairs of such coordination polyhedra connect through two longer bonds to form centrosymmetric Bi_2O_{12} dimers, which stack along the y-axis (yellow sphere-centred motifs in Figure 2a). These dimers are separated by infinite chains of edge-sharing ZnO_6 distorted octahedra (light blue polyhedra in Figure 2a). ZnO_4 and VO_4 tetrahedra share corners in an alternating manner to form chains which also run along the y-axis (Figure 2b). Finally, each ZnO_4 and VO_4 tetrahedron shares its two remaining vertices with two ZnO_6 groups, one above and one below it (Figure 2a), giving three-dimensional connectivity in the structure.

Table 1. Final crystallographic details for $BiZn_2VO_6$: space group P–1, unit cell parameters a = 6.88282(8) Å, b = 5.72906(6) Å, c = 8.9059(1) Å, α = 90.989(1)^o, β = 130.130(1)^o and γ = 99.548(1)^o, V = 261.170(6) Å^3

Label	**Site**	**x**	**y**	**z**	**U_{iso} (A)**
Bi1	2i	0.01108(31)	0.78508(25)	0.71693(19)	1.99(3)
Zn1	2i	0.99798(98)	0.73601(80)	0.08602(60)	1.99(3)
Zn2	2i	0.44086(89)	0.28142(61)	0.82736(57)	1.99(3)
V1	2i	0.4240(11)	0.77298(91)	0.61438(82)	1.99(3)
O1	2i	0.7578(30)	0.8569(26)	0.1034(24)	2.5(1)
O2	2i	0.7686(35)	0.8875(28)	0.8081(25)	2.5(1)
O3	2i	0.8200(32)	0.3785(26)	0.0088(22)	2.5(1)
O4	2i	0.6870(31)	0.3357(25)	0.6175(23)	2.5(1)
O5	2i	0.3206(31)	0.0172(27)	0.6223(22)	2.5(1)
O6	2i	0.6887(28)	0.4467(29)	0.3131(23)	2.5(1)

Table 2. Selected bond lengths and angles in $BiZn_2VO_6$

M – O bond	**M – O bond length (Å)**	**Selected bond angles around M (^{o})**
Bi1 – O1	2.195(13)	77.92(76)
Bi1 – O3	2.231(17)	77.99(76)
Bi1 – O2	2.417(29)	85.58(66)
Bi1 – O5	2.776(15)	91.29(50)
Bi1 – O6	2.778(23)	118.49(49)
Bi1 – O4	2.803(15)	139.41(54)
Bi1 – O5	2.904(24)	161.33(58)
Zn1 – O1	1.986(26)	88.11(81)
Zn1 – O3	2.050(15)	87.99(54)
Zn1 – O3	2.081(27)	86.74(56)
Zn1 – O4	2.190(14)	93.93(90)
Zn1 – O2	2.205(18)	173.90(70)
Zn1 – O2	2.225(15)	165.10(64)
Zn2 – O1	1.903(26)	108.76(90)
Zn2 – O3	1.945(17)	105.69(73)
Zn2 – O5	1.963(18)	110.83(89)
Zn2 – O6	1.969(17)	106.27(67)
V1 – O5	1.692(21)	106.3(12)
V1 – O6	1.719(22)	108.59(86)
V1 – O4	1.732(22)	114.85(84)
V1 – O2	1.789(17)	110.29(85)

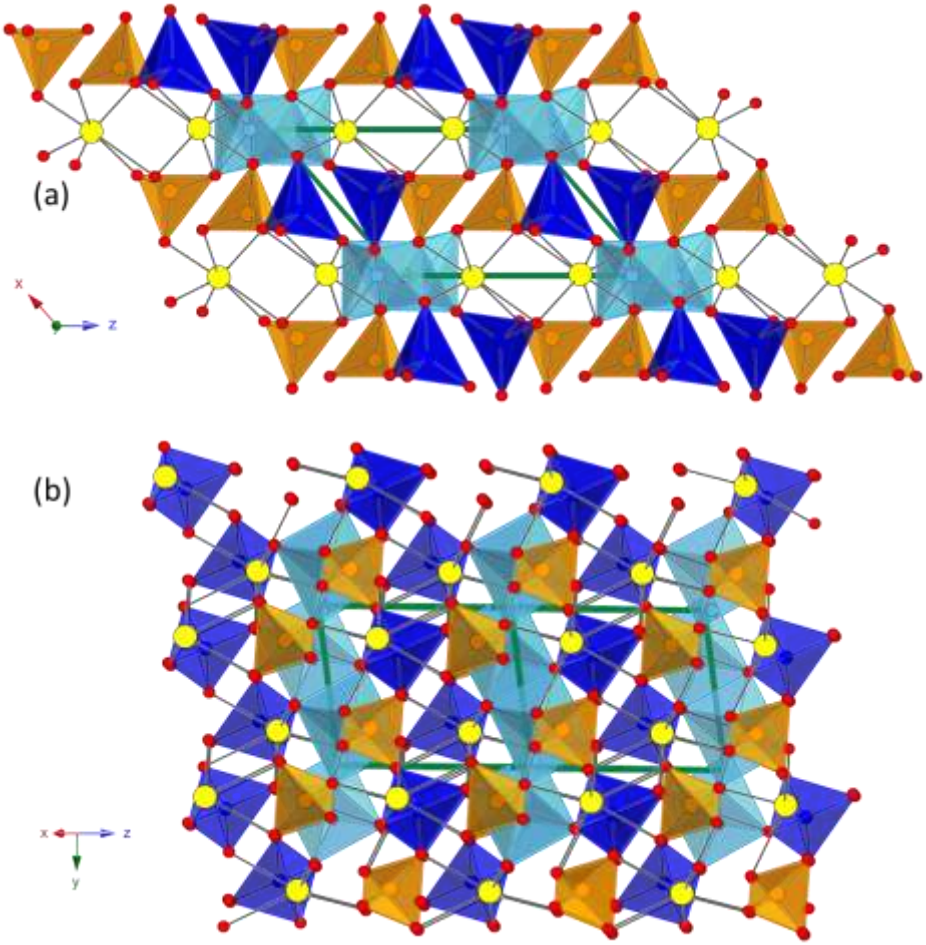

Figure 2. Polyhedral representation of the crystal structure of $BiZn_2VO_6$. The solid green line is the outline of the unit cell. Yellow spheres represent Bi atoms, red spheres O atoms; brown polyhedra are the VO_4 groups, dark blue polyhedra the ZnO_4 groups and light blue polyhedra the ZnO_6 groups.

Unit cell parameters and space groups for the seven known BiM_2VO_6 vanadates, along with the ionic radii of the relevant M^{2+} cations are summarised in Table 3. These are normally described as consisting of $(BiO_2)^{2-}$ chains, isolated VO_4 tetrahedra and interspersed M^{2+} cations. An alternative description, based on the edge-sharing of fluorite-like OBi_2M_2 tetrahedra and isolated VO_4 tetrahedra as the key structural building blocks, was proposed.[11] This enabled rationalisation of the different (but related) crystal structures adopted in terms of the VO_4 tetrahedra tilts relative to the arrangement in the highest symmetry variant and facilitated understanding of the structural phase transitions exhibited by some of these materials as a function of temperature.

Table 3. Structural characteristics of the BiM_2VO_6 phases (M = Pb, Ca, Cd, Mn, Zn, Mg, Cu).

M^{2+}	$r^{V}M^{2+}$ (Å)	Space group†	Unit cell parameters†							
			a (Å)	***b*** (Å)	***c*** (Å)	***α*** (°)	***β*** (°)	***γ*** (°)	***V*** (Å^3)	***V/fu*** (Å^3)
Pb	1.19*	Pn	7.715	29.082	5.849	90	94.2	90	1312	164
Pb§	1.19*	Pnma	9.443	12.074	6.038	90	90	90	688	172
Ca	1.00*	$Cmc2_1$	8.892	11.961	5.546	90	90	90	590	147
Cd	0.95*	$Cmc2_1$	8.644	11.459	5.646	90	90	90	559	140
Mn	0.75	Pnma	8.238	12.002	5.442	90	90	90	538	135
Zn	0.68	P–1	8.906	6.883	5.729	99.5	91.0	130.1	261	130
Mg	0.66	Pnma	7.916	12.247	5.443	90	90	90	528	132
Cu	0.65	$P2_1/n$	7.812	13.471	15.760	90	113.1	90	1525	127

†Crystallographic axes have been swapped relative to the published structures, if needed, to enable direct comparison. All space groups given are in the standard settings.
*Ionic radii for coordination number VI.
§High-temperature form.

Data in Table 3 summarise the space group and unit cell parameter data for the BiM_2VO_6 phases. Note that these have been determined under a variety of conditions (single crystal and powder, different temperatures), and are given for illustration of the structural relationships between different materials, rather than close detailed quantitative comparisons. The unit cell parameters of $BiZn_2VO_6$ do not exhibit cell metrics closely related to the rest of the BiM_2VO_6 series, and neither description of the related BiM_2VO_6 phases is applicable to it. This reflects the existence of different structural building blocks. For example, instead of infinite $(BiO_2)^{2-}$ chains, $BiZn_2VO_6$ contains discrete Bi_2O_{12} dimers; similarly, it does not contain fluorite-like slabs of edge-sharing OBi_2M_2 tetrahedra.

While it is not immediately clear why $BiZn_2VO_6$ adopts a structure type different from all other BiM_2VO_6 compounds, two further observations can be noted. For the six structurally related vanadates listed in Table 3 form, the phosphate analogues exist. In four of these cases (M = Ca, Cd, Mn, Mg), the vanadates and the phosphates are isostructural. In the remaining two cases (M = Pb, Cu), the vanadates adopt crystallographically more complex, lower symmetry structures related to those of the corresponding phosphates.

3.2 Investigation of solid solutions between $BiCu_2VO_6$ and $BiZn_2VO_6$

Given that both $BiCu_2VO_6$ and $BiZn_2VO_6$ depart from the basic orthorhombic BiM_2VO_6 structural aristotype and the similar ionic radii of Cu^{2+} and Zn^{2+}, we investigated the formation of $BiCu_{2-x}Zn_xVO_6$ mixed phases and their structural properties. In room temperature $BiCu_2VO_6$ there are six crystallographically independent Cu sites, four of which are 5-coordinate and two of which are 6-coordinate. In both cases, however, the coordination environments are better described as 4+1 and 4+2, since there are always four Cu–O short bond lengths of up to 2 Å, and an additional one about 2.3 Å long or two ranging from 2.5 and 2.8 Å.[6] We were therefore specifically interested in probing whether substituting either 1/3 or 2/3 of Cu atoms in $BiCu_2VO_6$ by Zn would result in the formation of single phase products with Cu/Zn cation ordering, which would lead to new, more complex superstructures.

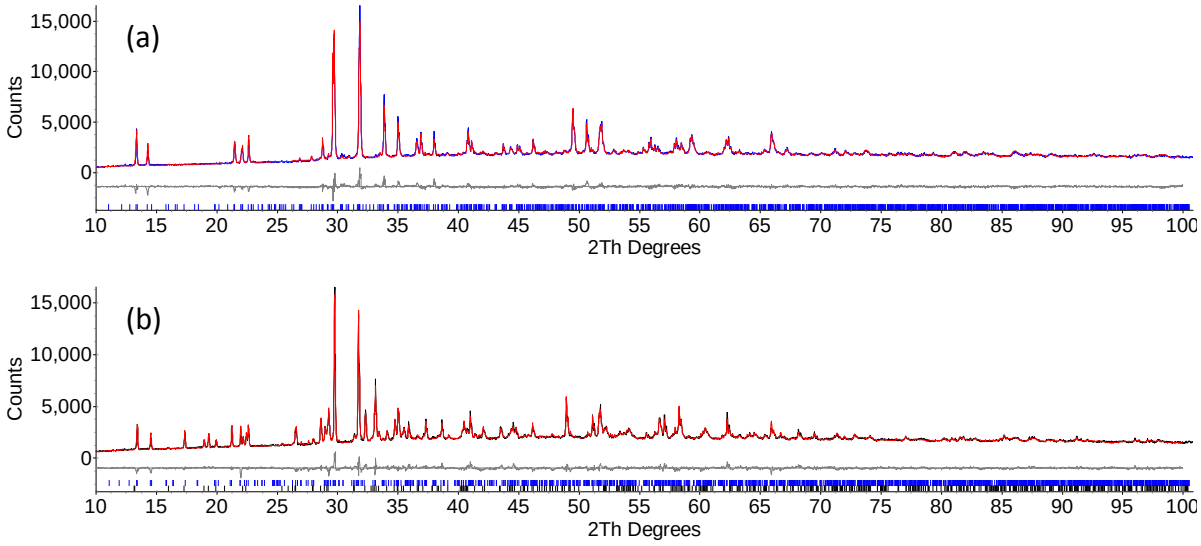

Figure 3. Rietveld plots for (a) $Bi(Cu_{2/3}Zn_{1/3})_2VO_6$; (b) a nominal $Bi(Cu_{1/3}Zn_{2/3})_2VO_6$ composition.

Figure 3a shows the Rietveld plot obtained for $Bi(Cu_{2/3}Zn_{1/3})_2VO_6$ by using the $BiCu_2VO_6$ structural model (R_{wp} = 4.97%). The agreement between the observed and the calculated patterns is excellent, confirming the presence of a single phase product; there is no evidence of significant structural change in this material relative to $BiCu_2VO_6$, apart from the unit cell volume increase. The unit cell parameters obtained for $Bi(Cu_{2/3}Zn_{1/3})_2VO_6$ are a = 13.5295(2) Å, b = 7.8633(1) Å, c = 15.8946(3) Å, β = 113.293(1)^o and V = 1553.16(5) Å^3, consistent with the incorporation of the slightly larger Zn^{2+} into the $BiCu_2VO_6$ structure. Figure 3b

shows the Rietveld plot for a nominal $Bi(Cu_{1/3}Zn_{2/3})_2VO_6$ composition. In this case, data analysis reveals phase separation, and the pattern can be fitted using two structural models, those of $BiCu_2VO_6$ and $BiZn_2VO_6$ (R_{wp} = 4.86%). The unit cell parameters for the phases two are a = 13.3519(4) Å, b = 7.8714(1) Å, c = 16.2327(3) Å, β = 113.882(3)^o and V = 1559.97(8) Å^3 for the former and a = 6.8737(3) Å, b = 5.7070(2) Å, c = 8.9137(4) Å, α = 91.254(3)^o, β = 129.957(3)^o and γ = 99.525(4)^o, V = 260.50(2) Å^3 for the latter. We conclude that no complex superstructures form in this system under the synthetic conditions used.

3.3 Electronic structure of $BiZn_2VO_6$

The DFT geometry optimisation resulted in unit cell parameters of $BiZn_2VO_6$ of a = 6.7829 Å, b = 5.5317 Å, c = 8.6658 Å, α = 91.0391°, β = 129.7831°, γ = 98.8854°. The optimised unit cell edges are smaller (by ~5%) than the experimental ones, which is commonly observed using the LDA method. The electronic band structure of yellow $BiZn_2VO_6$ is shown in Figure 4. Since most properties of a system are determined by the valence electrons, which mainly contribute to the band structures in the vicinity of Fermi level (set as E = 0 eV here), only the vicinity of Fermi level is shown in the figure. $BiZn_2VO_6$ is an indirect gap semiconductor, with a calculated indirect band gap E_g(i) ~ 1.6 eV. The direct band gap at **Z** (0 0 0.5) in the Brillouin zone E_g(d) is ~1.7 eV. The band gap determined experimentally by diffuse reflectance spectroscopy measurements on $BiZn_2VO_6$ is 2.4 eV [18], slightly larger than the calculated value. This result is not surprising, as the LDA calculations often underestimate the band gap of oxides.[27] The partial density of state (PDOS) plots for different atoms in $BiZn_2VO_6$ and total density of state (DOS) of $BiZn_2VO_6$ are shown in Figure 5. In the vicinity of the Fermi level, the main contribution to the valence band is from the O 2*p* orbitals, while the conduction band is formed mainly by the V 3*d* orbitals and the O 2*p* orbitals. Thus, the chemical properties of $BiZn_2VO_6$ are dominated by the V-O bond in the system.

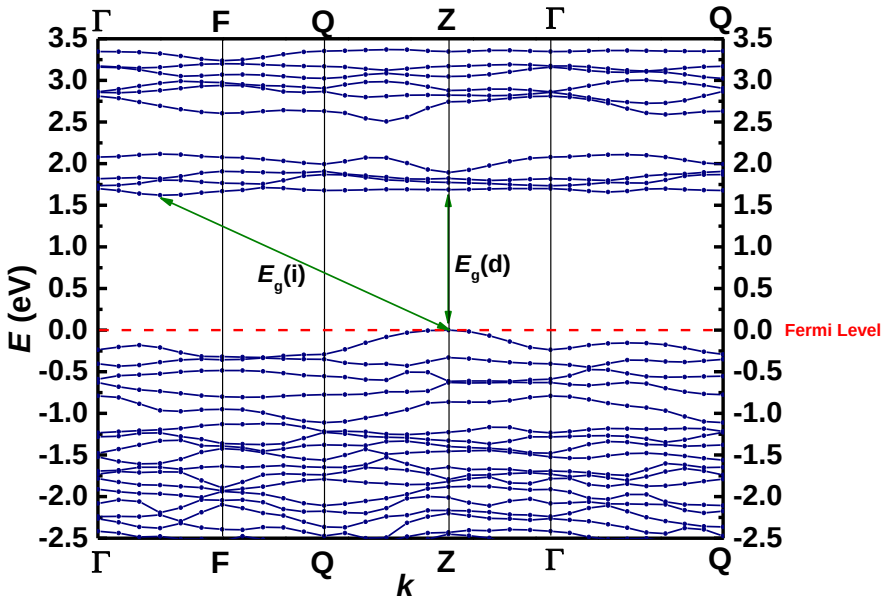

Figure 4. The electronic band structure of $BiZn_2VO_6$. The arrows indicate the indirect band gap E_g(i) and the direct band gap E_g(d); the Fermi level (dashed line) is set as E = 0 eV .

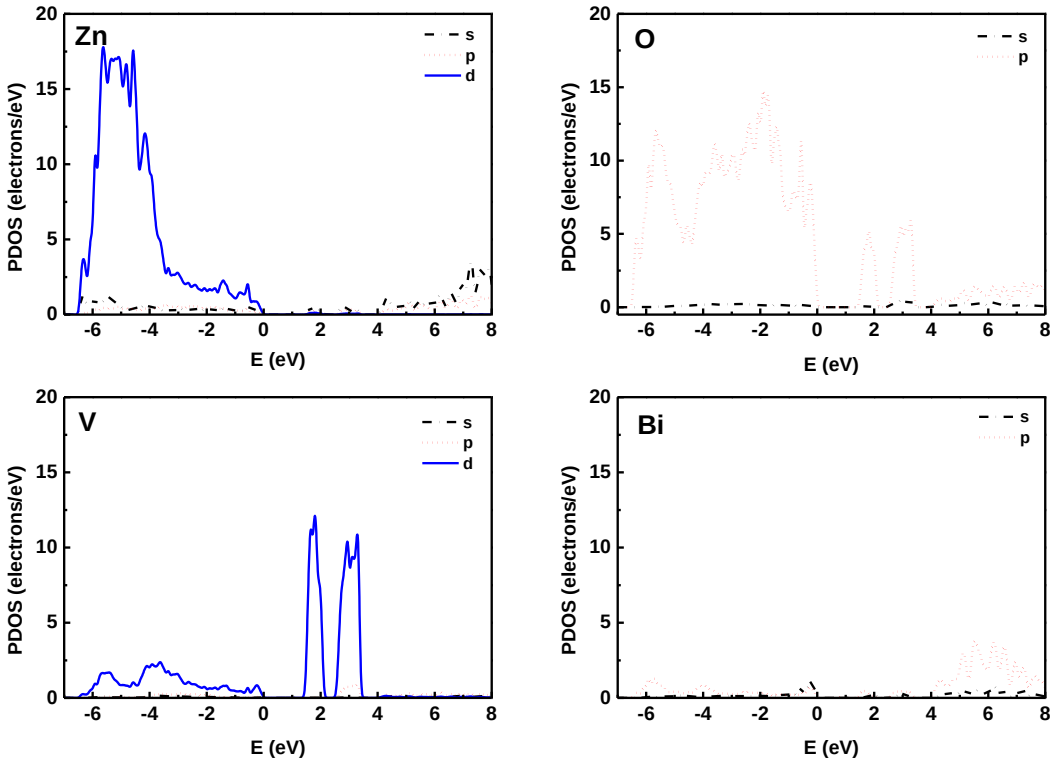

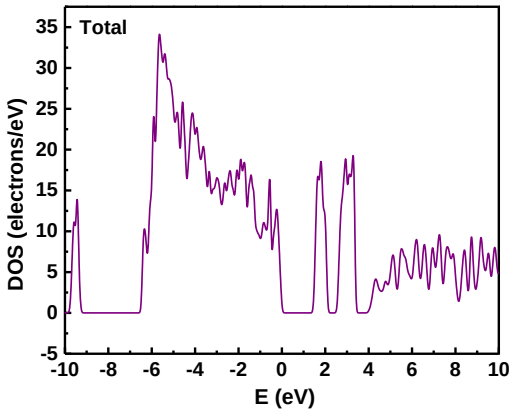

Figure 5. Partial density of state (PDOS) of different atoms and total DOS in $BiZn_2VO_6$. The Fermi level is set as $E = 0$ eV.

4. Conclusions

The crystal structure of bismuth zinc vanadate, $BiZn_2VO_6$, has been solved from laboratory powder X-ray diffraction data using the repeated minimisations from random starting values method. This material adopts an entirely new structure type, built up from corner- and edge-sharing ZnO_4 tetrahedra, ZnO_6 octahedra and VO_4 tetrahedra, and Bi_2O_{12} dimers. This is the only known member of the BiM_2AO_6 (M = Pb, Ca, Cd, Mn, Zn, Mg, Cu; A = V, P, As) family which doesn't appear to be structurally closely related to others.

Investigations into generating more complex BiM_2VO_6 superstructures by substituting 1/3 or 2/3 of Cu atoms in $BiCu_2VO_6$ by Zn showed that in the case of $Bi(Cu_{2/3}Zn_{1/3})_2VO_6$ a single-phase product was formed, adopting the $BiCu_2VO_6$ structure. Details of the Cu/Zn distribution over the crystallographic sites in this structure type cannot be probed by X-ray diffraction, due to insufficient contrast between the two species. In the case of nominal $Bi(Cu_{1/3}Zn_{2/3})_2VO_6$ composition, a two-phase product was obtained, as demonstrated by Rietveld analysis.

The electronic structure of $BiZn_2VO_6$, calculated by DFT methods, shows that this material is an indirect gap semiconductor, with a calculated band gap of 1.6 eV, which compares favourably to the experimentally measured value of 2.4 eV.

Acknowledgements

We would like to thank CAPES for an international postdoctoral fellowship to SEN.

References

[1] J.F. Huang, A.W. Sleight, *Journal of Solid State Chemistry* 100 (1992) 170-178.
[2] F. Abraham, M. Ketatni, G. Mairesse, B. Mernari, *European Journal of Solid State and Inorganic Chemistry* 31 (1994) 313-323.
[3] A. Mizrahi, J.P. Wignacourt, M. Drache, P. Conflant, *Journal of Materials Chemistry* 5 (1995) 901-904.
[4] A. Mizrahi, J.P. Wignacourt, H. Steinfink, *Journal of Solid State Chemistry* 133 (1997) 516-521.
[5] I. Radosavljevic, J.S.O. Evans, A.W. Sleight, *Journal of Solid State Chemistry* 137 (1998) 143-147.
[6] I. Radosavljevic, J.S.O. Evans, A.W. Sleight, *Journal of Solid State Chemistry* 141 (1998) 149-154.
[7] I. Radosavljevic, J.S.O. Evans, A.W. Sleight, *Journal of Alloys and Compounds* 284 (1999) 99-103.
[8] I. Radosavljevic, A.W. Sleight, *Journal of Solid State Chemistry* 149 (2000) 143-148.
[9] I. Radosavljevic, J.A.K. Howard, A.W. Sleight, *International Journal of Inorganic Materials* 2 (2000) 543-550.
[10] I.R. Evans, J.A.K. Howard, R.L. Withers, J.S.O. Evans, *Chemical Communications* (2001) 1984-1985.
[11] I.R. Evans, J.S.O. Evans, J.A.K. Howard, *Journal of Materials Chemistry* 12 (2002) 2648-2652.
[12] X. Xun, S. Uma, A. Yokochi, A.W. Sleight, *Journal of Solid State Chemistry* 167 (2002) 245-248.
[13] I.R. Evans, J.A.K. Howard, A.W. Sleight, *Solid State Sciences* 7 (2005) 299-302.
[14] I.R. Evans, S.W. Tao, J.T.S. Irvine, *Journal of Solid State Chemistry* 178 (2005) 2927-2933.
[15] O. Mentre, E.M. Ketatni, M. Colmont, M. Huve, F. Abraham, V. Petricek, *Journal of the American Chemical Society* 128 (2006) 10857-10867.
[16] C.S. Lue, S.C. Chen, C.N. Kuo, F.C. Chou, *Physical Review B* 80 (2009).
[17] T. Masuda, A. Zheludev, H. Kageyama, A.N. Vasiliev, *Europhysics Letters* 63 (2003) 757-763.
[18] H.M. Liu, R. Nakamura, Y. Nakato, *Electrochemical and Solid State Letters* 9 (2006) G187-G190.
[19] Z.X. Ding, Y.H. Fu, Z.P. Xie, Z.H. Li, *Materials Letters* 65 (2011) 460-463.
[20] H.M. Liu, R. Nakamura, Y. Nakato, *Chemphyschem* 6 (2005) 2499-2502.
[21] M. Bosacka, M. Kurzawa, I. Rychlowska-Himmel, I. Szkoda, *Thermochimica Acta* 428 (2005) 51-55.
[22] A.A. Coelho, J.S.O. Evans, I.R. Evans, A. Kern, S. Parsons, *Powder Diffraction* 26 (2011) S22.
[23] M.D. Segall, P.J.D. Lindan, M.J. Probert, C.J. Pickard, P.J. Hasnip, S.J. Clark, M.C. Payne, *Journal of Physics-Condensed Matter* 14 (2002) 2717-2744.
[24] G.S. Pawley, *Journal of Applied Crystallography* 14 (1981) 357.
[25] S. Kerman, B.J. Campbell, K.K. Satyavarapu, H.T. Stokes, F. Perselli, J.S.O. Evans, *Acta. Cryst. A* 68 (2012) 222.
[26] H.M. Rietveld, *Journal of Applied Crystallography* 2 (1969) 65-&.
[27] M.R. Dolgos, A.M. Paraskos, M.W. Stoltzfus, S.C. Yarnell, P.M. Woodward, *Journal of Solid State Chemistry* 182 (2009) 1964-1971.